Texture analysis and ultra high-frequency ultrasound in use for diagnosing Hirschsprung's disease

Jonathan Jedhammar (BME-20) & Sophia Klarén (BME-20)

***Abstract*—An investigation into the use of statistical texture analysis in combination with ultra high-frequency ultrasound for diagnosing Hirschsprung's disease (HD); An illness that manifests itself through the absence of ganglia cells in parts of the intestine. Current diagnostic techniques carry a higher risk of long-term consequences in newborns and children which enables a new avenue of research into new methods. This report delves into the use cases of the three statistical distribution types nakagami, skewness, and kurtosis. It has been found that these statistical texture parameters can differentiate between aganglionic and ganglionic tissues with high accuracy in longitudinal imaging and partly in transversal imaging. An interesting finding was that there is a difference between transversal and longitudinal images using Nakagami-m, which most likely is attributed to the direction of the muscle fibers. In longitudinal imaging, there is a significance of more than 99.9% when using the ratio and the difference between aganglionic and ganglionic tissues. Additionally, it is shown that our method can be used both for diagnostics and during surgery. However, further research is needed to validate these findings along a wide range of transducers and develop a reliable diagnostic method for HD using ultrasound.**

I. INTRODUCTION

HIRSCHSPRUNG'S DISEASE (HD) has, during the years 2018 to 2022, been investigated in 50 newborns at Lund University Hospital (SUS) by rectal biopsies and anography; of which 10 were ultimately diagnosed with HD. [1] Although the global prevalence is 1/5000, as many as 1/1000 newborns is estimated to be affected by the process of diagnosing. Both surgical biopsies, and the process of anesthetizing children to perform the biopsies, carry a higher risk of long-term consequences in newborns and children; One of which is brain injury. [2] Thus, current procedures enable our research into a novel technique that combines texture analysis with ultra high-frequency (UHF) ultrasound.

A. EPIDEMIOLOGY AND ANATOMY

1) Overview: Hirschsprung's disease, also known as Aganglionosis, is an intestinal disease that affects newborns. HD is characterized by the total lack of ganglia cells in the rectum, large intestine, and in some cases even the small intestine [3]. The condition arises in the developmental stage of the enteric nervous system and causes intestinal obstruction [4]. HD commences anorectally and progresses along the intestinal tract at different lengths depending on the severity of the disease. The lack of ganglia cells prevents the intestines from relaxing, causing difficulties to pass meconium, the infant's first stool. Furthermore, this often results in abdominal swelling and bloating, causing severe distress to the child [5].

Despite some genetic contributions, the primary cause of this disease remains unidentified. However, males tend to be affected at higher rates than females [3]. Furthermore, children with Down's Syndrome have a 100-fold higher risk of developing Hirschsprung's disease. [3]

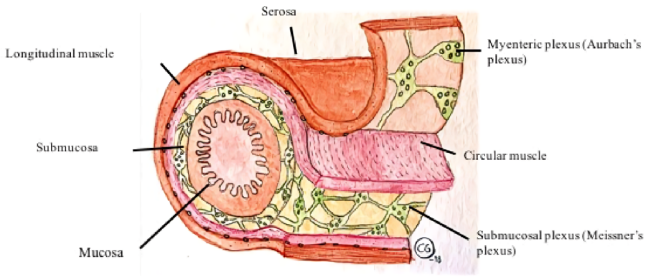

Figure 1: Tissue layers of the intestine [3]

2) Anatomy of the intestine: The intestinal wall is comprised of four distinct layers: the serosa, muscularis propria, submucosa, and mucosa, as illustrated in Fig. 1. The outermost layer, serosa, commonly referred to as the peritoneum, functions as a boundary between the intestine and the abdominal cavity. The muscular layer consists of two muscles, the circular and longitudinal muscles, also known as muscularis propria interna (MI) and muscularis propria externa (ME), respectively. In a healthy intestine ganglia cells are found in the myenteric (Aurbach's) and submucosal (Meissner's) plexuses, which are located between the muscularis interna and muscularis externa and in the submucosa, respectively. [6]

3) Diagnosis: Typical symptoms of Aganglionosis include trouble or inability to pass meconium, swollen abdomen, and vomiting [3]. Children that fail to pass meconium within their first 48 hours of life get examined for HD as well as differential diagnoses to HD [7]. In cases where Aganglionosis is suspected, an X-ray scan or anorectal manometry is typically

Report issued June 3, 2023
E-mail: so6713kl-s@student.lu.se, jo4805je-s@student.lu.se
Bachelor's thesis at the Department of Biomedical Engineering
Course: EEML05 - Kandidatarbete i klinisk innovation
Supervisor of Engineering applications: Tobias Erlöv, Institution of Biomedical Engineering
Supervisors of Medical applications: Pernilla Stenström, Christina Gráneli, Department of Pediatric Surgery, Skåne University Hospital
Swedish title: Analys av texturmått för användning av ultrahögfrekvent ultraljud vid diagnostisering av Hirschsprungs sjukdom

conducted to identify dysfunctional intestinal reflexes, indicative of HD [8]. Following the examinations are essential rectal biopsies from the intestine to dismiss or confirm Aganglionosis. As HD is life-threatening it requires immediate treatment, done by resecting the aganglionic part of the intestine. To achieve optimal outcomes from the surgery it is of great importance to resect all aganglionic tissue, while preserving most possible ganglionic tissue. Accordingly, an important part of the process is to as accurately as possible determine the correct resection length, by identifying the transition zone where aganglionic tissue proceeds to ganglionic tissue. The standard method for this today is by doing multiple biopsies from the intestinal wall until ganglionic tissue is found. However, this approach requires general anesthesia, which implies a risk to the child [2].

B. PREVIOUS RESEARCH

The diagnosis of Hirschsprung's disease using high-frequency ultrasound is a new area of research and therefore an established and absolute method is currently lacking. Previous research has examined possible methods that can identify differences between aganglionic and ganglionic tissues. A recent 2021 report examined differences in thickness between aganglionic and ganglionic tissue. [9] The article concluded that aganglionic tissue showed a decrease in the thickness of the intestinal wall. The difference turned out to be most significant in Muscularis Interna. Pernilla Stenström, Senior Physician in Pediatric Surgery, and Christina Gráneli, Specialist in Pediatric Surgery at Skåne University Hospital in Lund, have also found differences in homogeneity between tissues, as aganglionic tissue has an inhomogeneous texture compared to ganglionic tissue [1][10]. In order to implement a complete method for distinguishing aganglionic and ganglionic tissue, the difference must be statistically and objectively proven. This goal has yet to be achieved.

C. TEXTURE ANALYSIS AND APPLICATION

In this report, texture analysis will be investigated as a prospect for analysing ultrasound images of intestinal tissue. Texture analysis is a measurement of the inherent texture of the tissue as imaged by ultra high-frequency (UHF) ultrasound. Figure 2 shows an example of a UHF image.

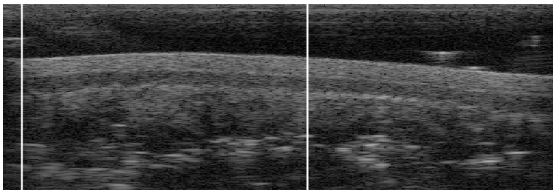

Figure 2: Longitudinal ultrasound image of ganglionic tissue layers

Depending on tissue type, the sound waves will scatter in different ways. The distribution of the echo captured by the receiver will therefore be different for various tissue types. The distribution parameters used in this work are nakagami-m, skewness, and kurtosis. Skewness has previously been used to characterize soft tissue [11] and Diffusion Kurtosis Imaging (DKI) has been used in multiple studies for imaging and characterizing different tissues.[12][13]. Nakagami distribution is useful for describing background scattering and speckles; It has been used in medical ultrasound applications for differentiating carcinogenic tissue from healthy tissue [14]. Below follows a definition for each of the distribution parameters used.

1) Skewness: Describes the asymmetry of a stochastic variable's distribution, and is given by Fischer's moment coefficient in equation 1. Skewness can have either negative or positive skew, or be normally distributed, as can be seen in Fig. 3, where E is the variance, μ is the mean, and σ is the standard deviation.

$$Skew(x) = E\left[\left(\frac{X-\mu}{\sigma}\right)^3\right] = \frac{\mu^3}{\sigma^3} \tag{1}$$

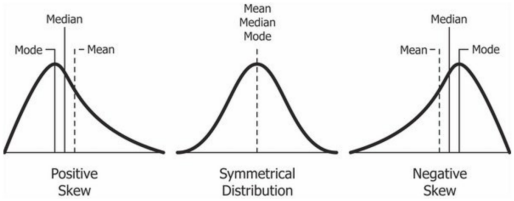

Figure 3: The three types of skewness and the relationship between median, mean value, and its mode. [15]

2) Kurtosis: Describes how sharp of an incline the distribution has. There are in simple terms three appearances: leptokurtic, platykurtic, and mesokurtic. A Leptokurtic distribution has a sharp incline and short tails, while a platykurtic distribution has a slow incline, with long tails. If the distribution resembles the normal distribution it is mesokurtic (see Fig. 4). The coefficient for Kurtosis is given by equation 2, where E is the variance, μ is the mean, and σ is the standard deviation.

$$Kurt(x) = E\left[\left(\frac{X-\mu}{\sigma}\right)^4\right] = \frac{\mu^4}{\sigma^4} \tag{2}$$

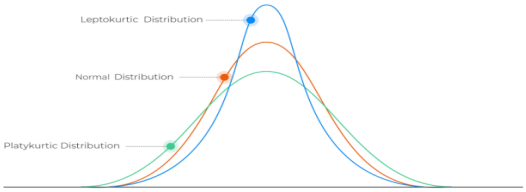

Figure 4: The three types of kurtosis. [16]

3) Nakagami: Describes the size and scattering of a distribution, and is given by:

$$Nak(x) = \frac{2m^m}{\Gamma(m)\Omega^m} * x^{2m-1} * e^{-\frac{m}{\Omega}x^2} \tag{3}$$

Where the m-parameter represents the size and Ω the

scattering of a variable.

The m parameter relates to Rayleigh distribution in the following way:

- Pre-Rayleigh for $0 \leq m \geq 1$,
- Rayleigh for $m = 1$ and
- Post-Rayleigh for $m > 1$

The m-parameter's effect on the distribution is displayed in Fig. 5.

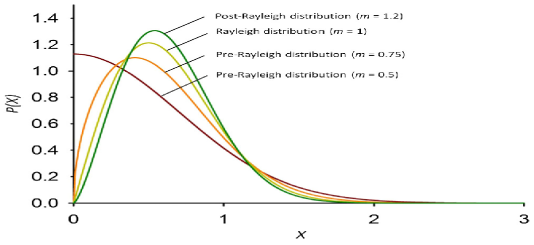

Figure 5: Graph of a Nakagami distribution with varying m-parameter [17]

D. THESIS

The method for diagnosing HD today is an extensive process that requires long waiting times and several invasive procedures. The protracted process risk causing psychological strain to both the children and their families due to increased responsibility for the child's health and of course, general parental concern [18]. In addition to the psychological stress, there is also physical stress caused by anesthesia, invasive surgery, and ionizing radiation affecting the child negatively, as well as permanently. Thus, there is a need for a more effective, in terms of time, and less invasive method for diagnosing. The aim of the study is to investigate the possibility to detect differences between aganglionic and ganglionic tissue through the means of UHF ultrasound and texture analysis.

E. AGENDA

The methods consist of three statistical distributions: nakagami, skewness, and kurtosis. The hypothesis being that the distributions would differ between Aganglionosisis and ganglionosis, but no differences between transversal and longitudinal images. Two main stochastic variables were created: one for ratio and one for difference, between aganglionic and ganglionic sample data, and other stochastic variables by means of creating a ratio between varying tissue layer types. Using statistical analysis the correlation between distribution data and ill tissue will be determined.

II. ETHICAL APPROVAL

The study was approved by the local ethical board (2017/769). Parental consents were obtained and patients were pseudo-anonymized (coded) for the analyses.

III. METHOD

A total of 19 patients contributed to the ultrasound images retrieved for the project by Stenström and Gráneli [10][1], taken with Vevo MD (FUJIFILM VisualSonics Inc., Toronto, Canada). The transducer attached to the ultrasound machine was UHF70, with an output frequency of 48 MHz. Nine (out of 19) patients were included in images taken transversely with respect to the length of the intestine, and 18 (out of 19) patients in images taken longitudinally. The mean age of the patients at the time of imaging was 34.8 ± 14 days.

Transversal and longitudinal images were taken on the removed intestine from the exterior of the intestine, on both ganglionic and aganglionic tissue. After retrieval, the images were analyzed in a Matlab program, originally created by Tobias Erlöv, a researcher at the Institution of Biomedical Engineering at Lund University, and further modified by us. The modifications implied changes made to the extraction process which eliminated the manual labor of changing the thickness of the submucosal tissue layer. The format of the images was B-mode.

The images were uploaded to the program, after which the boundaries between the different tissue layers were manually marked by entering a number of dots and allowing Matlab to join the dots together to form a line. For the third inner layer, the submucosa, three different depths of 0.18, 0.35, and 0.50 mm were used to potentially find an optimal depth. The regions between the layer boundaries could then be represented by areas, see Fig. 2 and Fig. 6. The areas were later used to calculate the amplitude distribution within the images for nakagami, skewness, and kurtosis in Matlab. The method was applied for both ganglionic and aganglionic tissue for all 19 patients.

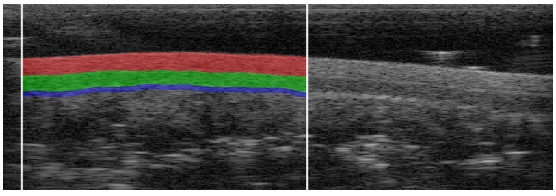

Figure 6: Longitudinal ultrasound image of ganglionic tissue layers, with areas of MI (green), ME (red), and SM (blue) marked as ROI (region of interest).

The difference and ratio between ganglionic and aganglionic values were determined as appropriate variables for further analysis of the distribution values. For the respective distributions, the difference and ratio were statistically tested to assess significance.

Moreover, additional variables were added at a later stage in order to further analyze differences between tissue layers. These variables would be defined as the ratio between the layer types. The created variables were: MI/ME, ME/SM-0.18 and ME/SM-0.35. The chosen layer ratios were decided upon findings from previous research. [1]

A. HYPOTHESIS TEST

The tests used for the statistical analysis were the Students T-test and Wilcoxon signed-rank test (further referred to as sign test), with the null hypothesis that there is an inequality between ganglionic and aganglionic tissue, and statistical significance of 5 percent. The alternative hypothesis being both values are equal. The choice of test depended on the appearance of the histograms, where normally distributed histograms were tested with a T-test, and non-normal distributed histograms were tested with Wilcoxon's signed-rank test/sign test.

B. MUCOSAL IMAGING

Additional measurements were done for transversal images taken of the intestine from the inside out (transversal mucosal). Although the number of patients in this category is only five, the analysis was thought to be interesting. The reason for this is based on the idea that this method could be used help to diagnose HD during surgery with a transducer that is insertable into the rectum, and thus imaging the intestine extending from the mucosa out to ME.

IV. RESULTS

A. LONGITUDINAL VS. TRANSVERSAL IMAGING

The box plots displayed in Fig. 7 present patient-specific data of the variable Nakagami-m for both transversal and longitudinal images in each respective tissue layer. Each data point is marked as a red dot. Points marked with crosses are outliers.

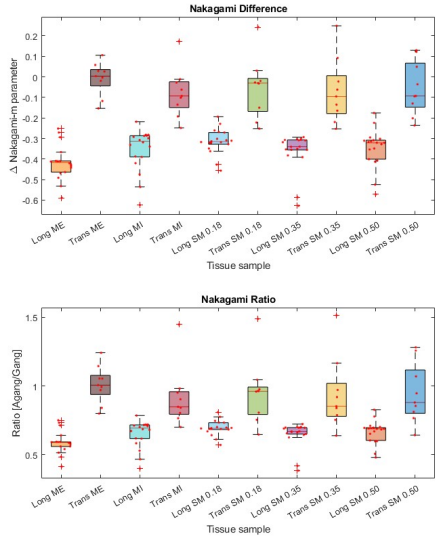

Figure 7: Comparison between longitudinal and transversal values of ratio and difference for Nakagami-m parameter in each tissue layer.

Skewness and kurtosis showed results differing from 0 (for the variable difference) and 1 (for the variable ratio), whereas Nakagami-m presented a greater difference than skewness and kurtosis, hence being the sole graph displayed.
As seen in Fig. 7, when the tissue is imaged in the longitudinal direction the Nakagami m-parameter shows a greater difference and ratio between ganglionosis and aganglionosis compared to when imaged in the transverse direction. Hence, going forward results will mostly disregard transversal images in favor of longitudinal ones.

B. DISTRIBUTIONS OF LONGITUDINAL IMAGING

Nakagami texture analysis displays the major difference in general (meaning: disregarding unique patient-patient relevance) can be found in MI and submucosa (using a thickness of 0.18 mm) as seen in Fig. B.1. Moreover, the data for the variables ratio and difference for ME, MI, and submucosa (0.18 mm), in Fig. B.1, showcase favorable values.
Logarithmic skewness shows a similar result for use in ME, MI, and submucosa (0.18 mm) which is visualized in Fig. B.3. However, it should be noted that in general (disregarding patient-patient specific data) only submucosa (0.18 mm) generated the best results with the least overlap to 0 and 1 for difference and ratio respectively.
Texture analysis using logarithmic kurtosis overlaps the values 0 and 1 on all occasions (general use, difference, and ratio) as seen in Fig. B.2.

C. DISTRIBUTIONS OF TISSUE LAYER RATIOS

As visualized in Fig. 8 there are differences made visible using ratio between layer types. Some data are very uniform, such as in Nakagami-m, while other data is distributed along an interval.

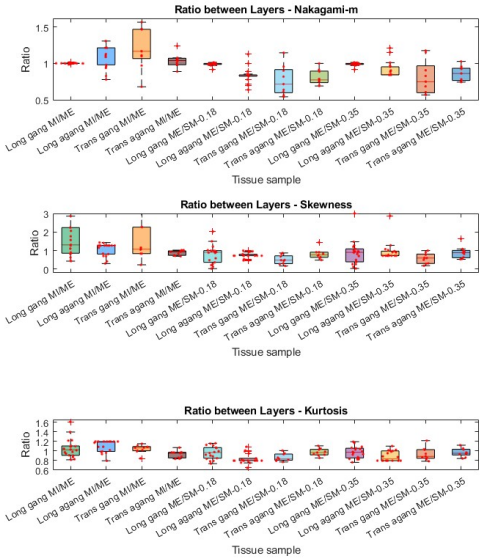

Figure 8: Ratio between given layer types and ganglionic/aganglionic tissue. Given layers are divided into distribution types: Nakagami-m [T], logarithmic skewness [M], and logarithmic kurtosis [B]. The data is patient-specific.

D. HYPOTHESIS TESTS

With regards to whether the various data points from the distribution types were normally distributed or not, a t-test or a sign test was performed which is displayed in table A.I for longitudinal images, in table A.II for transversal images, and in table A.III for transversal mucosal images.

The p-values from the hypothesis test for longitudinal and transversal images are presented in table II and I. The significant values, that are $p \leq 0.05$, are put in **bold** and colored green.

Table I: p-value from hypothesis test for each tissue layer and distribution type of **longitudinal** images.

Tissue layer	Variable	Nakagami	Skewness	Kurtosis
MI	Ratio	**<0.00001**	0.2379	0.4807
	Difference	**<0.00001**	0.2379	0.4807
ME	Ratio	**<0.00001**	0.0963	0.8145
	Difference	**<0.00001**	0.0551	0.8145
SM 0.18 mm	Ratio	**<0.00001**	**0.0309**	**0.0013**
	Difference	**<0.00001**	**0.0309**	**0.0013**
SM 0.35 mm	Ratio	**<0.00001**	0.0963	**0.0191**
	Difference	**<0.00001**	0.0963	**0.0185**
SM 0.50 mm	Ratio	**<0.00001**	**0.0023**	**0.0309**
	Difference	**<0.00001**	**0.0023**	**0.0309**

For Nakagami distribution all tissue types show great significance, while for skewness and kurtosis significant values were found in submucosa only.

As visualized in table II, for transversal images the majority of the significant values stem from Muscularis Interna and submucosa with 0.18 mm depth. The corresponding significant layers for longitudinal images are submucosa with 0.18 and 0.50 mm depth, where 100% of the tests confirmed significance which can be seen in table I.

Table II: p-value from hypothesis test for each tissue layer and distribution type of **transversal** images.

Tissue layer	Variable	Nakagami	Skewness	Kurtosis
MI	Ratio	**0.0391**	0.5078	**0.0391**
	Difference	0.0888	0.2772	**0.0142**
ME	Ratio	0.8139	0.5078	0.7627
	Difference	1	0.5078	0.6547
SM 0.18 mm	Ratio	0.1797	**0.0078**	**0.0391**
	Difference	0.1797	**0.0078**	**0.0391**
SM 0.35 mm	Ratio	0.1797	**0.0402**	0.5078
	Difference	0.1797	0.1797	0.5078
SM 0.50 mm	Ratio	0.5078	0.5078	1
	Difference	0.2497	0.0605	1

For transversal mucosal images, no significance could be attained, as can be seen in table III.

Table III: p-value from hypothesis test for each tissue layer and distribution type of **transversal mucosal** images.

Tissue layer	Variable	Nakagami	Skewness	Kurtosis
MI	Ratio	1	0.2500	1
	Difference	1	0.2500	1
ME	Ratio	0.3750	0.3750	1
	Difference	0.3750	0.0504	1
SM 0.18 mm	Ratio	1	0.3750	0.3433
	Difference	1	0.3750	0.2785

Tests conducted on the tissue layer ratios, however, have many significant results which can be seen in table IV below. Most are found in kurtosis where 4/6 tests showed a significant result, while 3/6 in Nakagami-m and 2/6 in skewness.

Table IV: p-value from hypothesis test for each tissue layer ratio and distribution type of **longitudinal** and **transversal** images.

Tissue ratio	Imaging type	Nakagami	Skewness	Kurtosis
MI/ME	Longitudinal	**0.0963**	0.2379	0.4636
	Transversal	0.1439	0.1797	**0.0391**
ME/SM-0.18	Longitudinal	**<0.0001**	0.8145	**0.0309**
	Transversal	0.6101	**0.0219**	**0.0106**
ME/SM-0.35	Longitudinal	**0.0075**	0.4807	**0.0309**
	Transversal	0.5078	**0.0432**	0.5972

V. DISCUSSION

Table I and II display values which confirm that both longitudinal and transversal imaging can segment between different tissue types and aganglionic and ganglionic tissue. Our findings of uniformity and statistical significance give way for use in both diagnostics and during surgery by means of replacing the use of biopsy, hence eliminating current practices of higher risk.

For diagnostics, both Nakagami-m and tissue ratios can be used. Nakagami-m has no overlap, and tissue ratios due to distinct intervals and high significance. Furthermore, the tissue ratios of transversal imaging make for a more convenient design of anal probing[19][1].

We were unable to determine an optimal submucosal thickness with accuracy, however, the data points to it being 0.18 - 0.35 mm as 0.50 mm could at times overlap with the mucosa which causes a high significance.

A. LONGITUDINAL VS. TRANSVERSAL IMAGING

Nakagami-m longitudinal images produced highly significant values, while transversal had overlap (see Fig.7). The results are inconclusive for skewness and kurtosis. Thus suggesting that longitudinal imaging is superior for diagnosing HD. This finding is somewhat surprising as one would expect that sound interacting with the tissue would be independent of the angle of imaging. However, this could be caused by differences in

the orientation of muscle fibers and other anatomical structures in the intestinal wall. It is also possible that the image of the intestine could be reconstructed or processed differently depending on the angle of the transducer, or a differing number of patients included in longitudinal and transversal images.

B. MUCOSAL IMAGES

Results for transversal mucosal images indicate no dissimilarity between the ganglionic and aganglionic tissue. However, further analysis of a larger dataset is required.

C. TISSUE LAYER RATIOS

Comparing to the box plot in Fig. 8 it is seen that some ratios are very uniform and have a very small interval. Despite the overlap, the difference in interval and uniformity can be further utilized for segmentation purposes. Moreover, table IV further confirms these findings. This is of great value for diagnosing HD since it does not rely upon a comparison between ganglionic and aganglionic tissue.

D. TRANSDUCER SPECIFIC RESULTS

While the result is robust compared to previous research's amplitude response segmentation [9], it has still only been tested on one specific transducer using a center frequency of 48 MHz. With this knowledge in mind, more research is required for wide usage between various ultrasound machines and transducers of the same center frequency.

E. ACCURACY OF HYPOTHESIS TESTS

In table A.II and table A.I the chosen tests for each layer and its respective distributions are shown. The sign test is the dominating test, as it was used in approximately 82% of all tests. As opposed to the T-test, the sign test is non-parametric. This means the test makes few assumptions about the distribution, which may come at the expense of the statistical power of the test. However, it ensures the applicability of the statistical analysis in this report.

The successful methods have an inherently low risk of false positives, while still applying false negatives of unknown certainty. In other words, they have a low risk of false diagnosis and an unknown risk of removing more healthy intestinal tissue than needed.

F. SUSTAINABLE DEVELOPMENT

The current method for diagnosing HD requires access to ultrasound- and x-ray machines as well as tools and skills for surgically performing biopsies. From an environmental point-of-view, surgeries most often result in waste from non-recyclable goods that contributes to the strain on the environment. Using the new method of diagnosing HD with only UHF ultrasound, the number of biopsies required could decimate to zero.

Radiology clearly affects the environment and sustainability as it consumes a substantial amount of energy and is a considerable producer of greenhouse gasses [20]. Furthermore, there is a safety concern regarding the ionizing radiation it produces that affects the child. It is therefore important to terminate this part of the process of diagnosing, to achieve a more sustainable method. The ultrasound itself causes minimal effects on the environment, in terms of consuming energy, emitting CO_2, and affecting human health from pollution [21].

The present method for diagnosing one child with HD in Sweden requires an average of one anography, 1.8 biopsies, and 1.5 hours of surgery. The cost of this amounts to 33.480 Swedish crowns (SEK) [22],[23]. Implementation of a method using only one ultrasound examination could reduce the costs to 4840 SEK, implying a reduction of 28.640 SEK for each child. This corresponds to a yearly minimum saving of 716.000 SEK in Sweden, counted on 25 children diagnosed with HD.

Moreover, the procedure allows for less time spent in surgery. These eliminations and reductions will in turn make diagnosing HD using UHF ultrasound environmentally, as well as more economically sustainable; While at the same time ensuring safe medical practice for children.

G. ETHICS

All children included in the retrieval of images are vulnerable as their information is used and published. As HD in the majority of the cases is discovered in the newborn's first year of life, the children are unable to give consent to their data being used in this project. However, retrieving and using the images is done so under consent from each child's parents, under the awareness that the images are being used in the current study performed by our supervisors. As for the integrity of the patients, all were pseudo-anonymized using a patient code system, see II.

VI. CONCLUSION

By means of texture analysis, it has been concluded that there is a significant difference between the textures of ganglionic and aganglionic tissue of Hirschsprung's Disease. This presents a hopeful avenue for distinguishing tissue both during and prior to surgery, which could potentially reduce the surgical duration and minimize risks and discomfort for pediatric patients. However, additional research is necessary to establish a definitive method for diagnosing HD.

VII. ACKNOWLEDGEMENTS

A most special thanks to our supervisor Tobias Erlöv for being our main support and for guiding us along the entire journey. Thank you for always encouraging us to try new ideas.

We would also like to extend our sincerest gratitude to Pernilla Stenström and Christina Gráneli for having played a major role in our clinical learning process, and for being

dedicated in our journey.

The dataset used has partly been ranked and selected by Tebin Hawez (researcher at Lund University Hospital). This has been a great help to filter out images with high resolution from the dataset.

The workload has been equally divided between the two authors. For previous research on HD, as well as background research, both authors have done close to equal shares. As the project developed however, the research was divided into parts of marking data and programming. Sophia Klarén has marked the majority of all tissue types, as well as performed the statistical analysis, while Jonathan Jedhammar changed the Matlab software used, and created new scripts for various analyses and plots.

BIBLIOGRAPHY

[1] S. Pernilla, "Interview with pernilla stenström", 2023.

[2] R. The Children's Hospital at Westmead Sydney Children's Hospital, Y. P. Kaleidoscope Children, and Families, *Anaesthesia and risk in infants*, (Last accessed: 2023-05-17), 2017. [Online]. Available: https://www.schn.health.nsw.gov.au/fact-sheets/anaesthesia-and-risk-in-infants.

[3] G. Christina, *Hirschsprung's disease. physical outcome and innovations*, (Last accessed: 2023-04-26), 2019. [Online]. Available: https://lucris.lub.lu.se/ws/portalfiles/portal/55664119/e_spik_ex_graneli.pdf.

[4] e. a. Fransson E, *Diagnostic efficacy of rectal suction biopsy with regard to weight in children investigated for hirschsprung's disease*, (Last accessed: 2023-04-26), 2022. DOI: doi.org/10.3390/children9020124.

[5] T. P. Butler Tjaden NE, *The developmental etiology and pathogenesis of hirschsprun disease*, (Last accessed: 2023-04-26), 2013. DOI: 10.1016/j.trsl.2013.03.001.

[6] W. R. Reed K.K, *Review of the gastrointestinal tract: From macro to micro*, (Last accessed: 2023-04-26), 2008. DOI: doi.org/10.1016/j.soncn.2008.10.002.

[7] T. L. Gomella, M. D. Cunningham, F. G. Eyal, and D. J. Tuttle, "No stool in 48 hours", in *Neonatology: Management, Procedures, On-Call Problems, Diseases, and Drugs, 7e*. New York, NY: McGraw-Hill Education, 2013. [Online]. Available: accesspediatrics.mhmedical.com/content.aspx?aid=1107527910.

[8] K. R. Ambartsumyan L Smith C, *Diagnosis of hirschsprung disease*, (Last accessed: 2023-04-26), 2020. DOI: 10.1177/1093526619892351.

[9] O. H. Vernersson Alvina, "Användning av ultrahögfrekvent ultraljud under operation av hirschsprungs sjukdom", Tech. Rep., 2021, (Last accessed: 2023-04-19). [Online]. Available: https://bme.lth.se/fileadmin/biomedicalengineering/Courses/Projekt_i_klinnovation/Total_Klinnovation2021.pdf.

[10] G. Christina, "Interview with christina gräneli", 2023.

[11] A. M. Mahmoud, O. M. Mukdadi, B. Teng, and S. J. Mustafa, *High-resolution quantitative ultrasound imaging for soft tissue classification*, (Last accessed: 2023-04-27), 2011. DOI: 10.1109/MECBME.2011.5752071.

[12] e. a. Kulich BA M, *Chapter 3 - imaging findings in mild traumatic brain injury*, (Last accessed: 2023-04-28), 2019. DOI: https://doi.org/10.1016/B978-0-12-812344-7.00003-0.

[13] e. a. Archana Vadiraj M, *Ivim-dki with parametric reconstruction method for lymph node evaluation and characterization in lymphoma: A preliminary study comparison with fdg-pet/ct*, (Last accessed: 2023-04-27), 2023. DOI: https://doi.org/10.1016/j.rineng.2023.100928.

[14] e. a. Mamou J, *Three-dimensional high-frequency backscatter and envelope quantification of cancerous human lymph nodes*, (Last accessed: 2023-04-27), 2012. DOI: 10.1016/j.ultrasmedbio.2010.11.020.

[15] D. Jain, *Relationship between mean and median under different skewness*, (Last accessed: 2023-05-08), 2018. [Online]. Available: https://commons.wikimedia.org/wiki/File:Relationship_between_mean_and_median_under_different_skewness.png.

[16] A. Kumar, *Descriptive statistics – key concepts & examples*, (Last accessed: 2023-05-08), 2023. [Online]. Available: https://vitalflux.com/descriptive-statistics-key-concepts-examples/.

[17] J.-J. Lin, J.-Y. Cheng, L.-F. Huang, Y.-H. Lin, Y.-L. Wan, and P.-H. Tsui, "Detecting changes in ultrasound backscattered statistics by using nakagami parameters: Comparisons of moment-based and maximum likelihood estimators", *Ultrasonics*, vol. 77, pp. 133–143, 2017.

[18] e. a. Abbasiasl H, *Explaining the care experiences of mothers of children with hirschsprung's disease: A qualitative study*, (Last accessed: 2023-04-27), 2021. DOI: 10.1177/2333794X211015520.

[19] M. Evertsson, "Interview with maria evertsson", 2023.

[20] e. a. Chua LB A, *The environmental impact of interventional radiology: An evaluation of greenhouse gas emissions from an academic interventional radiology practice*, (Last accessed: 2023-05-08), 2021. DOI: 10.1016/j.jvir.2021.03.531.

[21] e. a. Martin BS M, *Environmental impacts of abdominal imaging: A pilot investigation*, (Last accessed: 2023-05-08), 2018. DOI: https://doi.org/10.1016/j.jacr.2018.07.015.

[22] P. Wendel, *Regionala priser och ersättningar för södra sjukvårdsregionen*, (Last accessed: 2023-05-15), 2022. [Online]. Available: https://sodrasjukvardsregionen.se/download/regionala-priser-och-ersattningar-for-sodra-sjukvardsregionen-2023/?wpdmdl=33055&masterkey=5ByR7kQ6lD6oDyCTddTALXUg70XZL4RAyPMXiF6YK0a4Jvt6isQzss6TxlkyicMqbmdoDMSX4aUqpSnpIdIi2UGKo_Hn2OfWE97omkWb7rU.

[23] *Pris 2023 - region skåne samt landstingen blekinge, södra halland, kronoberg, klinisk genetik, patologi och molekylär diagnostik*, (Last accessed: 2023-05-15), 2023. [Online]. Available: https://vardgivare.skane.se/siteassets/2.-patientadministration/avgifter-och-prislistor/prislistor/labmedicin/rs---fillistning/klinisk-genetik-patologi-och-molekylardiagnostik---for-region-skane-och-sodra-sjukvardsregionen.pdf.

APPENDIX A
TABLES

Table A.I: Choice of hypothesis test in the statistical analysis used for respective tissue layer and statistical distribution type of **longitudinal** images.

Tissue layer	Variable	Nakagami	Skewness	Kurtosis
MI	Ratio	Sign test	Sign test	Sign test
	Difference	Sign test	Sign test	Sign test
ME	Ratio	Sign test	Sign test	Sign test
	Difference	Sign test	Sign test	Sign test
SM 0.18 mm	Ratio	Sign test	Sign test	Sign test
	Difference	Sign test	Sign test	Sign test
SM 0.35 mm	Ratio	Sign test	Sign test	T-test
	Difference	Sign test	Sign test	T-test
SM 0.50 mm	Ratio	Sign test	Sign test	Sign test
	Difference	Sign test	Sign test	Sign test

Table A.II: Choice of hypothesis test in the statistical analysis used for respective tissue layer and statistical distribution type of **transversal** images.

Tissue layer	Variable	Nakagami	Skewness	Kurtosis
MI	Ratio	Sign test	Sign test	Sign test
	Difference	T-test	T-test	T-test
ME	Ratio	T-test	Sign test	T-test
	Difference	Sign test	Sign test	T-test
SM 0.18 mm	Ratio	Sign test	Sign test	Sign test
	Difference	Sign test	Sign test	Sign test
SM 0.35 mm	Ratio	Sign test	T-test	Sign test
	Difference	Sign test	Sign test	Sign test
SM 0.50 mm	Ratio	Sign test	Sign test	Sign test
	Difference	T-test	T-test	Sign test

Table A.III: Choice of hypothesis test in the statistical analysis used for respective tissue layer and statistical distribution type of **transversal mucosal** images.

Tissue layer	Variable	Nakagami	Skewness	Kurtosis
MI	Ratio	Sign test	Sign test	Sign test
	Difference	Sign test	Sign test	Sign test
ME	Ratio	Sign test	Sign test	Sign test
	Difference	Sign test	T-test	Sign test
SM 0.18 mm	Ratio	Sign test	Sign test	T-test
	Difference	Sign test	Sign test	T-test

Table A.IV: Choice of hypothesis test in the statistical analysis used for respective tissue layer and statistical distribution type of **longitudinal** and **transversal** images. **NOTE:** All tests in this table are two-sample tests.

Tissue ratio	Imaging type	Nakagami	Skewness	Kurtosis
MI/ME	Longitudinal	Sign test	Sign test	T-test
	Transversal	T-test	Sign test	Sign test
ME/SM-0.18	Longitudinal	Sign test	Sign test	Sign test
	Transversal	T-test	T-test	T-test
ME/SM-0.35	Longitudinal	Sign test	Sign test	Sign test
	Transversal	Sign test	T-test	T-test

APPENDIX B
BOX PLOTS

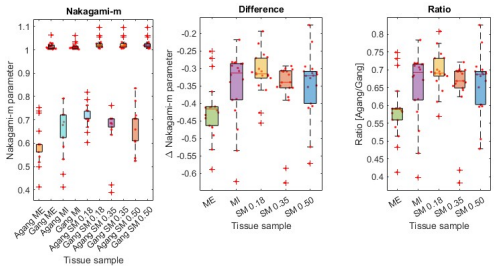

Figure B.1: Nakagami m-parameter value [in L], the variable of difference [in M], and the variable of ratio [in H] of different tissue samples. All values represent longitudinal images.

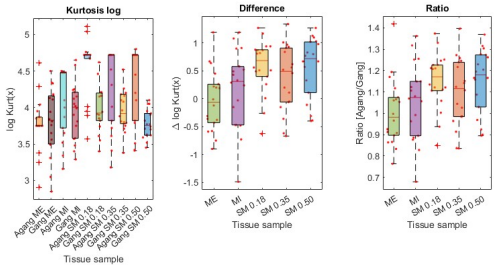

Figure B.2: Logarithmic kurtosis coefficient value [in L], the variable of difference [in M], and the variable of ratio [in H] of different tissue samples. All values represent longitudinal images.

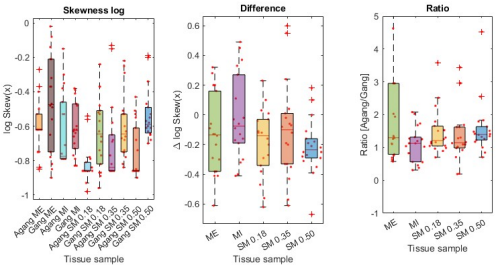

Figure B.3: Logarithmic skewness coefficient value [in L], the variable of difference [in M], and the variable of ratio [in H] of different tissue samples. All values represent longitudinal images.